Formation of acicular ferrite and influence of vanadium alloying

K. He and D. V. Edmonds

The effect of vanadium microalloying in promoting a tough, acicular ferrite microstructure in C–Mn steels has been investigated. The microstructure obtained consisted of fine interlocking ferrite plates and was indistinguishable from acicular ferrite developed in steel weld metals, apparently from the intragranular nucleation of ferrite at inclusions. A number of variables were examined in high purity experimental steels including composition and heat treatment conditions, and related to a metallographic examination of the microstructure by high resolution microanalytical transmission electron microscopy and surface analysis. A comprehensive study of the inclusions in the steels, containing different ratios of oxygen and nitrogen concentration, did not find any significant evidence that inclusion assisted nucleation was the sole determining factor in producing acicular ferrite. Moreover, no evidence could be found to relate vanadium alloying to significant vanadium nitride precipitation, either separately, or associated with the inclusions. Thus, in the present steels, any possible alternative influence of vanadium on intragranular ferrite nucleation is not obscured by effects associated with the inclusion population. The vanadium concentration appeared to be the most important influence in developing an acicular ferrite microstructure in these experimental steels, and this is not inconsistent with previous reports in the literature of a beneficial 'vanadium effect'. Evidence for vanadium segregation in the microstructure was found, which may be related to the effect of vanadium in encouraging the formation of acicular ferrite. Even when there is good evidence that inclusions are responsible for intragranular ferrite nucleation (as, for example, in steel weld metals), a 1 : 1 inclusion–ferrite relationship has been difficult to establish. Thus, even an inclusion activated nucleation theory is likely to require additional intragranular ferrite formation without inclusion assistance, such as sympathetic or autocatalytic nucleation, and this could be reflected in the present study by vanadium atom clustering facilitating an alternative intragranular ferrite nucleation mechanism.

MST/4958

The authors are in the Department of Materials, University of Leeds, Leeds LS2 9JT, UK (D.V.Edmonds@leeds.ac.uk).
Manuscript received 15 January 2001; accepted 22 May 2001.

Introduction

Acicular ferrite is the term used to describe a microstructure comprising fine interwoven ferrite laths or plates, first recognised in high strength, low alloy (HSLA) steel weld metals. This fine interlocking structure was found to be a desirable microstructure in low carbon steel weldments because it showed improved toughness over that of other transformation products, such as conventional bainite.[1,2] The early recognition of the importance of weld metal oxygen content,[3] followed by metallographic observations of acicular ferrite plates in contact with inclusions (for example, Ref. 4), provided persuasive evidence for the development of the acicular ferrite microstructure by intragranular nucleation of ferrite at weld metal inclusions, rather than at grain boundaries, which otherwise would lead to coarser, and less tough, microstructures. However, the exact mechanism responsible for acicular ferrite nucleation at inclusions remains unclear.[4–11]

There is also some evidence to suggest that not every ferrite crystal is nucleated by an inclusion; experimental studies based on measurement and comparison of the number density of ferrite plates and inclusions found that only about one in 10 plates was inclusion nucleated.[12] This is, qualitatively, readily apparent from many of the published micrographs relating to this topic, although, clearly, it is acknowledged that quantitative interpretation of such observations is difficult to qualify because of stereological considerations, which estimate that only ~ 10% of ferrite plates would be expected to be observed in association with an inclusion (although even this is not absolute evidence that the inclusion nucleated the plate).[13]

Consequently, it has been necessary to invoke the possibility of a secondary nucleation event to transform the austenite between inclusions. In this respect, it has been known for some time that so called 'sympathetic nucleation' of Widmanstätten ferrite plates, one on another, can occur.[14] Indeed, there is support for acicular ferrite as a form of Widmanstätten ferrite,[4,6,15] although this is not universally accepted, and an alternative description offered is that acicular ferrite is intragranularly nucleated bainite.[16–18] In the latter case, however, experimental evidence has been presented to suggest that autocatalytic nucleation of bainitic ferrite plates plays a part in the development of the acicular ferrite microstructure.[19]

The above developments in steel weld metals have been followed by several attempts to reproduce a tough acicular ferrite microstructure in plate steels, by imitating the perceived inclusion activated formation mechanism and inoculating with oxygen and other suitable alloying additions: Ti oxides,[20] Si–Mn oxides,[21] and MnS+ CuS inclusions[22] have all been considered effective for inducing intragranular nucleation of ferrite in parent plate steels.

A less noted effect from studies of acicular ferrite in weld metals is that vanadium additions may enhance the acicular ferrite microstructure and improve toughness,[23–27] although it is difficult to separate the conflicting effects of other alloying elements, weld heat input and cooling rate, and carbonitride precipitation. A preliminary metallographic study in high purity C–Mn steels showed that a vanadium addition increased the amount of fine interlocking acicular ferrite microstructure at the expense of coarse bainite, and this, apparently, appeared not to be solely dependent upon inclusion assisted intragranular nucleation of ferrite.[28] Consequently, the study reported in the present

paper was conceived principally to confirm whether vanadium additions could influence austenite decomposition beneficially in this way, thus providing an alternative microalloying route to the production of tough ferritic microstructures in plate steels.

Experimental procedures

Experimental steels were prepared based on Fe–0·1C–0·25Si–1·2Mn (wt-%) with nominal vanadium contents between 0 and 0·5 wt-%. High purity elements were used to make 50 g ingots in an arc melting furnace under a partial pressure of argon gas, or 980 g ingots in a vacuum induction furnace. Table 1 gives the compositions of the experimental steels. The two different melting routes resulted in two sets of oxygen/nitrogen ratios; ingots from arc melting had lower oxygen and higher nitrogen concentrations, while ingots from induction melting had higher oxygen but lower nitrogen concentrations.

Heat treatments were conducted either in sealed silica tubes or under an argon atmosphere. The small, arc furnace melts were homogenised at 1150°C for 100 h. Specimens were austenitised at 1050, 1150, and 1200°C for 20–180 min (giving an austenite grain size of ~ 200 μm), followed by continuous cooling to room temperature at cooling rates of approximately ~ 4–11 K s^{-1} over the temperature range 800–500°C. Cooling rates were measured using a Pt–13%Rh thermocouple, spot welded to the specimen, with temperature recorded by a data logger.

Standard techniques were used to prepare specimens for examination by optical microscopy, and quantitative metallography was carried out using point counting methods. Specimens for transmission electron microscopy (TEM) were first mechanically ground to a thickness of 100 μm from thin slices, and then electropolished in a twin jet unit using an electrolyte of 10% perchloric acid, 30% 2-butoxyethanol, and 60% ethyl alcohol, at 20 mA, 15 V and about −10°C. Examination by TEM and scanning transmission electron microscopy (STEM) microanalysis were carried out in a Philips CM 20 instrument, with Oxford Instruments UTW EDX attachment, operating at 200 kV. Energy dispersive X-ray spectral processing was carried out using Oxford Instruments ISIS software, with the supplied virtual standards package. Secondary ion mass spectrometry (SIMS) was carried out on a VG Escalab Mk I with a gallium source, operated at 10 kV with 1 nA current and scanning areas typically 20–50 μm^2.

Hardness tests were conducted on a Vickers machine using a 10 kg load. An average from 10 readings was recorded. Impact testing was carried out using a balanced Hounsfield impact test machine. Cylindrical V notched test specimens, 8 mm in diameter and 44 mm in length, were machined from slightly larger blanks, and heat treated by austenitising at 1200°C for 40 min and continuously cooling at ~ 7 K s^{-1}.

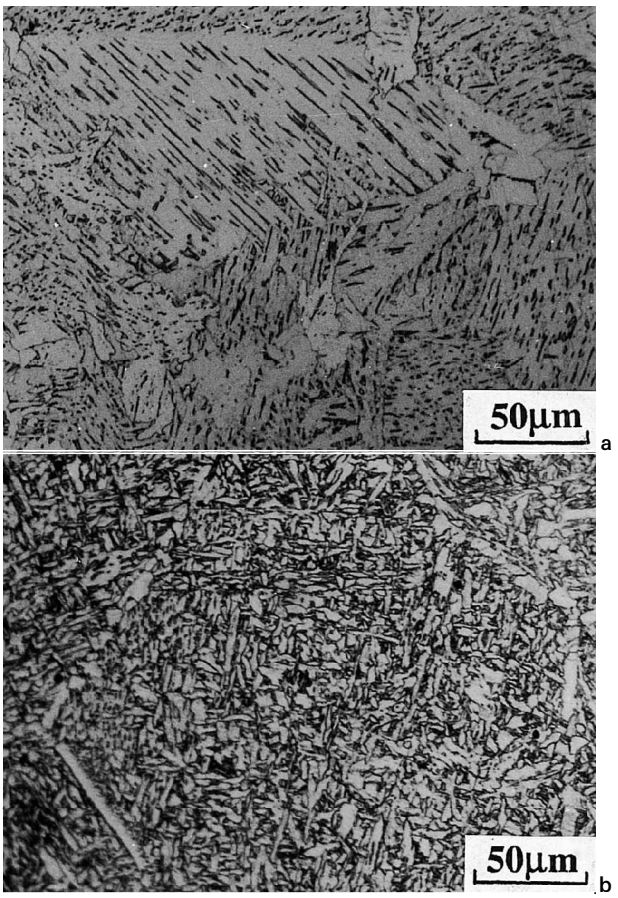

a V free steel (AA-00); b V containing steel (AA-25)

1 Typical optical microstructures

Results

VANADIUM ALLOYING EFFECTS

In general, the vanadium free steels consisted mainly of coarse bainite with grain boundary allotriomorphic ferrite, as shown in Fig. 1*a*. The vanadium treated steel microstructures, in contrast, contained a significant proportion of acicular ferrite (Fig. 1*b*), up to 80% depending upon the vanadium content and heat treatment. The lowest nominal (wt-%) vanadium addition of 0·1%V resulted in an acicular ferrite proportion of ~ 50%, mainly at the expense of bainite, and a further increase to ~ 80% was achieved by 0·25%V addition. The amount of acicular ferrite obtained by increasing the vanadium content to 0·5%V remained at ~ 80% (Fig. 2).

Figure 3 illustrates a region of mixed microstructure in a vanadium containing steel with 0·25%V addition. The prior

Table 1 Compositions of experimental steels, wt-%

Code	C	Si	Mn	P	S	Al	Cu	N	Ti	V	O	Fe
Argon arc melting												
AA-00	0·06	0·30	1·15	<0·005	0·005	<0·05	<0·05	0·015	<0·05	<0·05	0·009	Bal.
AA-10	0·11	0·27	1·16	<0·005	0·005	<0·05	<0·05	0·012	<0·05	0·09	0·007	Bal.
AA-25	0·09	0·31	1·21	<0·005	0·005	<0·05	<0·05	0·016	<0·05	0·23	0·007	Bal.
AA-50	0·10	0·27	1·20	<0·005	0·005	<0·05	<0·05	0·019	<0·05	0·48	0·010	Bal.
Vacuum induction melting												
V-00	0·07	0·24	1·51	0·006	0·003	<0·05	<0·05	0·010	0·05	<0·05	0·021	Bal.
V-10	0·09	0·28	1·33	<0·005	0·002	<0·05	ND*	0·004	ND*	0·10	0·011	Bal.
V-25	0·05	0·24	1·42	0·009	0·005	<0·05	0·51	0·007	<0·05	0·24	0·016	Bal.
V-40	0·10	0·18	1·38	0·008	0·003	<0·05	0·05	0·003	ND*	0·41	0·010	Bal.

*ND not determined.

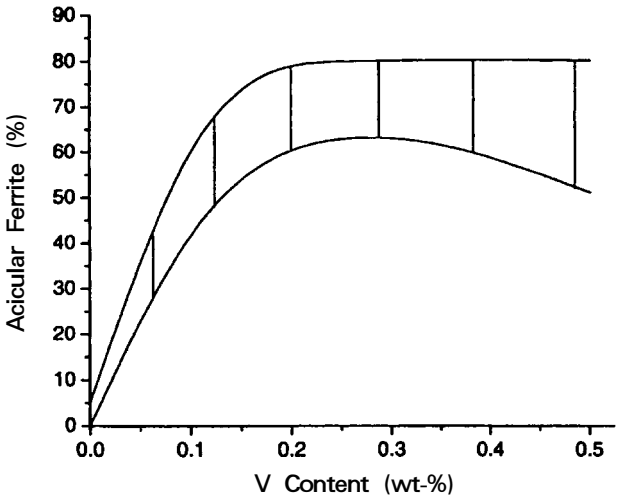

2 Proportion of acicular ferrite versus V content

austenite grain boundaries are associated with a layer of allotriomorphic ferrite, found in all of the experimental steels with or without vanadium addition, although it was noted qualitatively that this layer appeared thinner and sharper in the vanadium containing steels. It can also be seen from Fig. 3 that regions of coarse bainitic structure could still develop from this grain boundary ferrite.

It can be noted from Table 1 that the carbon concentration in the vanadium free steels was, on average, lower than in the vanadium treated steels. However, an increase in acicular ferrite content was produced (for example, compare steel V-25 with steel V-00) even when the carbon concentration was decreased. The appearance of acicular ferrite in the vanadium treated steels does not appear, therefore, to be the consequence of any variation in carbon concentration.

The acicular ferrite crystals appear to have formed independently, at large angles to each other, resulting in an interwoven, or cross-hatched, appearance. The overall microstructural form of the acicular ferrite was indistinguishable from that frequently recorded for low carbon steel weld metals. The same could be said for the appearance of the acicular ferrite as observed by TEM (Fig. 4*a*). The individual ferrite crystals displayed a broad range of morphologies around a general plate shape; some plates were acicular with sharp tips, but others were more angular or blocky, while some had a quite irregular shape. The apparent size of the individual acicular ferrite crystals was approximately 5–10 μm in length and 1–4 μm in width. By interrupting the continuous cooling transformation with a water quench it could be shown, as in Fig. 4*b*, that the larger, first formed plates restricted the growth of those formed subsequently, which probably accounts for the apparent mixture of morphologies, from the more acicular, first formed plates to shorter stunted plates, where lengthening had been restricted. Figure 4*c* also shows that the bainitic form of ferrite in these steels was identifiably different, in the TEM, from the acicular ferrite form.

Little evidence of precipitation of fine V(C,N) in the grain boundary ferrite, by an interphase precipitation mechanism

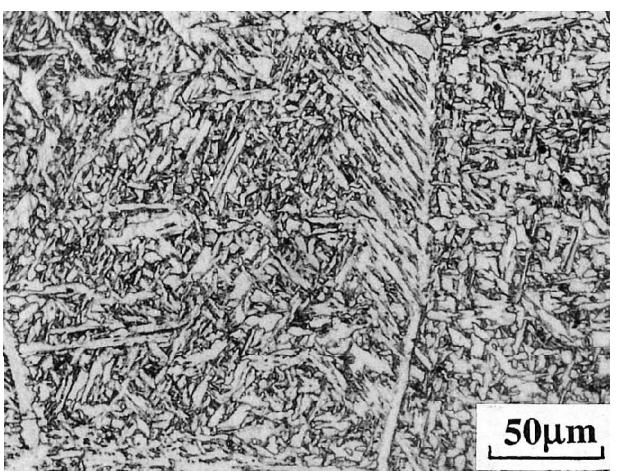

3 Mixed microstructure of grain boundary ferrite, bainitic ferrite, and acicular ferrite in V containing steel (V-25) (optical)

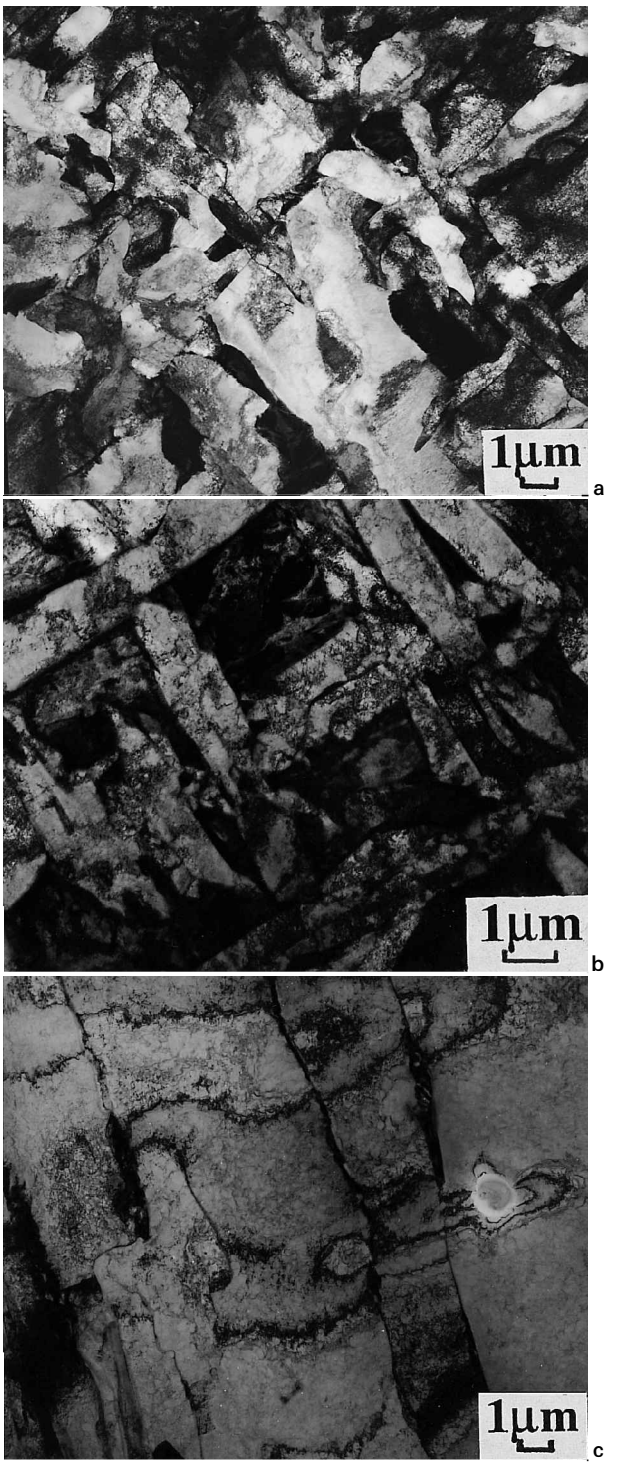

a,b V containing steel (AA-25); c V free steel (AA-00)

4 Typical TEM microstructures

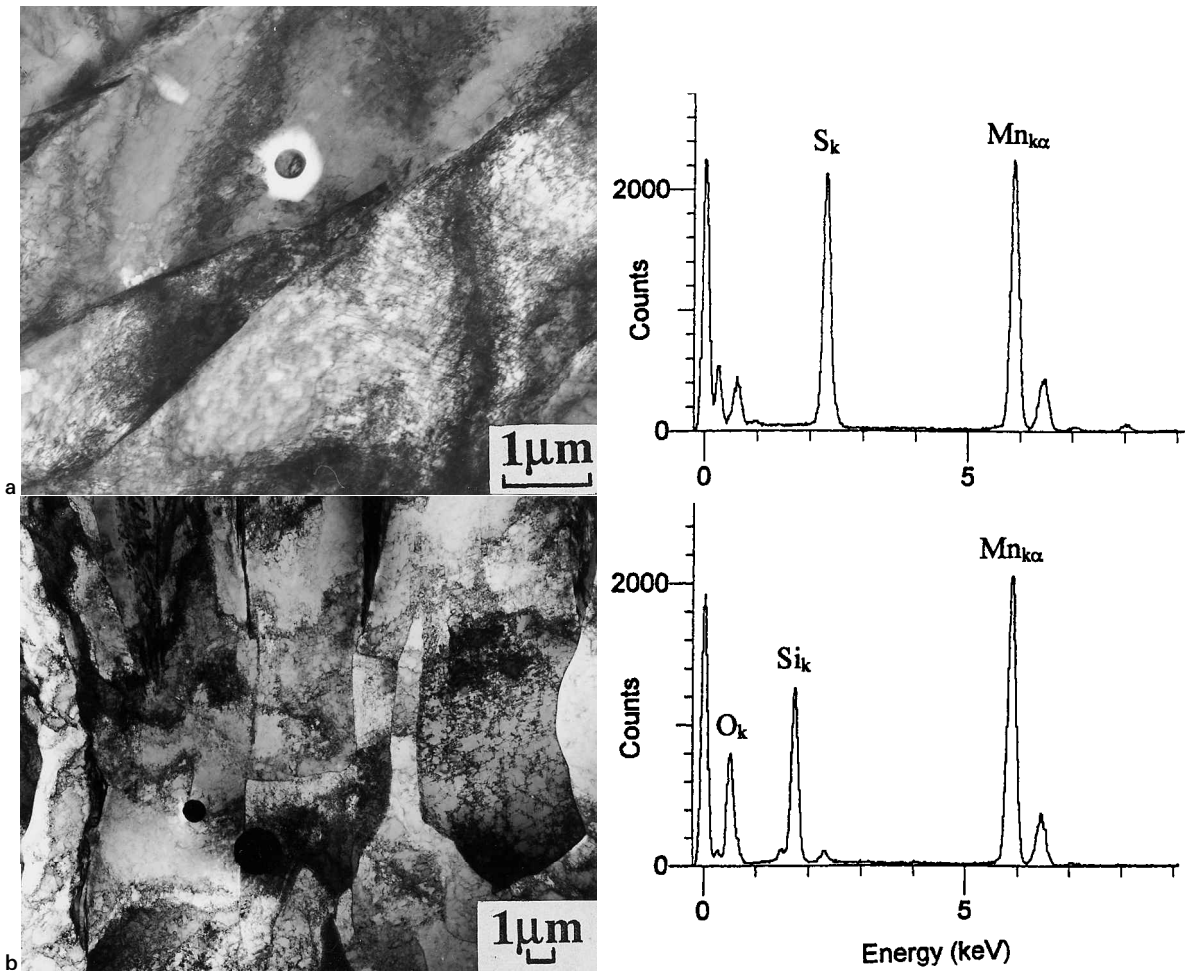

a low oxygen steel (AA-00); b high oxygen steel (V-00)

5 Inclusions (TEM) and EDX spectra

or otherwise, as reported previously,[28] was observed, but some larger undissolved V(C,N) particles (>0·1 μm) were found scattered in the matrix, especially in the 0·5%V steel.

EFFECTS OF HEAT TREATMENT CONDITIONS

A range of austenitising treatments were examined: 1050, 1150, and 1200°C for 20–180 min, giving an austenite grain size of ~ 200 μm. This was followed by continuous cooling to room temperature at cooling rates of ~ 4 and ~ 11 K s^{-1} over the temperature range 800–500°C. A tendency to produce some polygonal ferrite at the lower austenitising temperatures was noted, which increased with increased vanadium content and reduced cooling rate. To avoid this for all of the vanadium levels used in the present work, an austenitising temperature of 1150°C at 0·25%V and the higher cooling rate of 11 K s^{-1} at 0·5%V were required. However, this ferrite, although polygonal rather than acicular, displayed a fine ferrite grain size of about 5–10 μm, approximately equivalent to the length of the acicular ferrite plates.

INCLUSION EFFECTS

Microanalytical TEM found a number of different types of non-metallic inclusions, larger than 0·1 μm, present in all of the experimental steels, despite the high purity melting conditions employed. The basic nature of the inclusions varied according to the laboratory melting route used and the resulting oxygen concentration differences.

In the steels with a lower oxygen content (Table 1, argon arc melting), the majority of the inclusions were identified as MnS (Fig. 5*a*). These MnS inclusions were found in the vanadium free steel and also in the bainite regions of the vanadium containing steels. It thus appears likely that these sulphide inclusions were not an effective nucleant for acicular ferrite. Other inclusions identified were copper sulphide inclusions, and MnS inclusions with a trace of copper sulphide, possibly a composite of the two.

In the low oxygen–high nitrogen steels (Table 1, argon arc melting) containing vanadium, a composite of MnS inclusion plus V(C,N) phase was occasionally observed (Fig. 6). It has been suggested[29,30] that vanadium can enhance the nucleation potential of inclusions by precipitation of VN at the inclusion surface; the nitride nucleates the ferrite with which it produces a low energy interface. However, slower cooling rates than employed in the present work are generally required to induce this effect, accounting for the general absence of V(C,N) precipitation observed in the present study. More than 40 inclusions were examined, and in all cases the inclusions were contained within a single ferrite crystal. No examples were found whereby an inclusion had nucleated more than a single ferrite variant.

In the steels that contained higher oxygen contents (Table 1, vacuum induction melting), the inclusions were mainly Si–Mn oxides (Fig. 5*b*). The population of oxide inclusions was much higher than that of the sulphides. The Si–Mn oxides could be effective in nucleating ferrite plates, as they were sometimes observed in contact with more than one ferrite plate variant, as shown in Fig. 7*a*. However, most of the inclusions still had a 1:1 inclusion–ferrite relationship. Moreover, many Si–Mn oxides were also found in bainite plates (Fig. 7*b*). No vanadium was detected

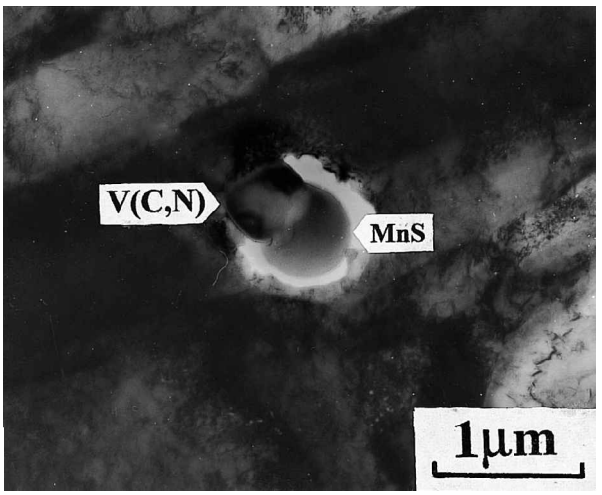

6 Complex inclusion of MnS+ V(C,N) within ferrite plate in V containing steel (AA-50) (TEM)

at any oxide or MnS inclusions from the results of ~ 50 EDX analyses in these high oxygen – low nitrogen steels. In addition, no differences in acicular ferrite microstructure or content were apparent between the steel series with high oxygen concentrations and those containing less oxygen.

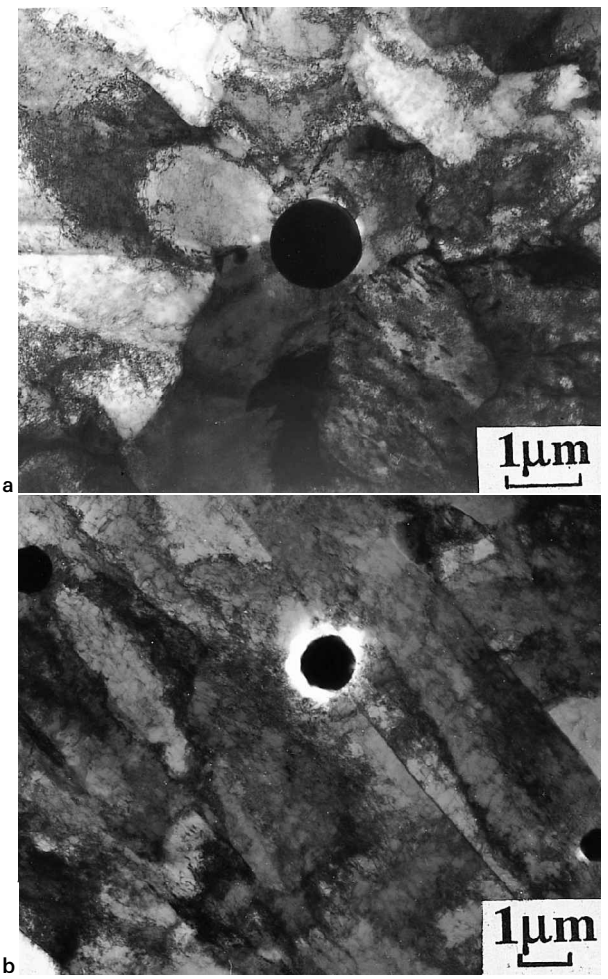

a surrounded by several ferrite plates in V containing steel (V-25); b within bainite of V free steel (V-00)

7 Si–Mn oxide inclusions (TEM)

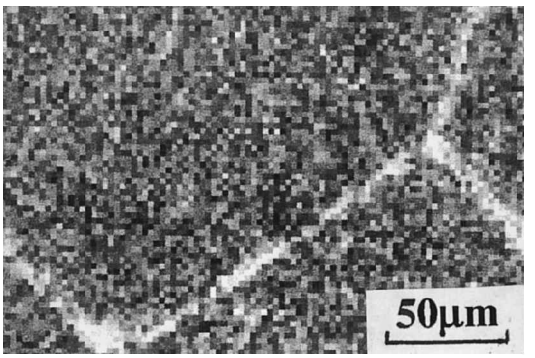

8 Secondary ion mass spectrometry (SIMS) image showing V concentrated at prior austenite grain boundaries (AA-50)

VANADIUM SEGREGATION

In the absence of visible vanadium precipitation associated with grain boundary ferrite or inclusions, the distribution of vanadium was examined by microanalytical techniques. Secondary ion mass spectrometry imaging, with a spatial resolution of 200 nm, was employed to examine the vanadium concentration at the prior austenite grain boundaries. This technique has the advantage of examining grain boundaries using a bulk specimen, in which these boundaries are more readily located and identified. Figure 8 shows clear evidence of vanadium segregation at prior austenite grain boundaries as identified by SIMS maps of positive vanadium ions (mass unit = 51 amu). When it was certain that a prior austenite grain boundary had been located by high resolution TEM, no evidence of vanadium precipitation was ever observed.

To investigate whether there was also any evidence of residual segregation within the acicular ferrite microstructure, indicative of vanadium segregation within the original austenite grains, a microanalytical STEM method[31] was used. The resolution of SIMS was insufficient for this experiment. An attempt was made to measure the vanadium concentration within acicular ferrite plates and at the boundary between them, these representing two distinctly separate and identifiable locations within the fully transformed microstructure. The thin foil was tilted, to orient a chosen ferrite plate boundary plane parallel to the electron beam. The analysis was carried out using a reduced area STEM – EDX technique with a 'letterbox' scanned area width of 20 – 75 nm, to measure the vanadium concentration in a well defined volume containing the ferrite plate grain boundary $[V]_b$ as well as that in the neighbouring ferrite grain $[V]_\alpha$ (Fig. 9). The excess vanadium concentration at the boundary Γ_b^V can be expressed as

$$\Gamma_b^V = [([V]_b/[Fe]_b) - ([V]_\alpha/[Fe]_\alpha)]N_\alpha^{Fe}\, w$$

where N_α^{Fe} is the site density of iron in a ferrite plate, which is 84·949 nm^{-3}, and w is the dimension of the analysis area perpendicular to the interface, which is slightly bigger than the scanned area because of beam broadening. One monolayer of iron sites in a ferrite plate is defined as $(84{\cdot}949)^{2/3} = 19{\cdot}32$ atoms/nm^2. Therefore, the extent of vanadium segregation can be expressed in terms of monolayers of vanadium sites at the boundary i.e. monolayer of vanadium sites = Γ_b^V/monolayer of iron sites. Table 2 gives the results of this analysis, which indicate a definite segregation of vanadium in the acicular ferrite microstructure, as compared between ferrite plate interiors and plate boundaries. The plate boundaries were richer in vanadium, although the segregation varied from boundary to boundary, and also from place to place on the ferrite plate grain boundary.

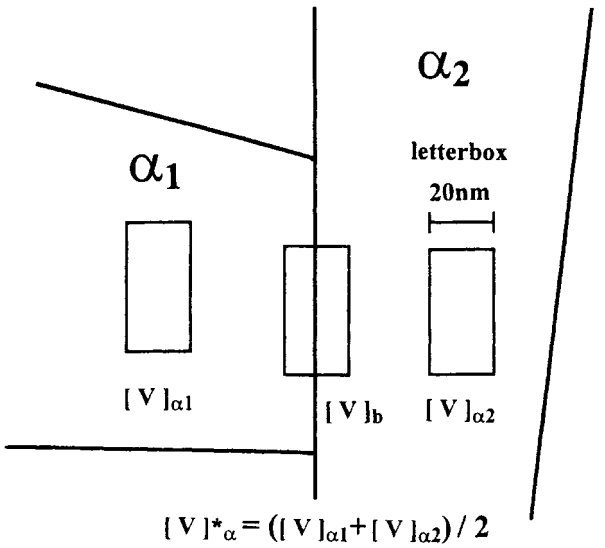

9 Schematic diagram illustrating position of 'letterbox' scanned area

MECHANICAL PROPERTIES

Hardness measurements and balanced Hounsfield impact tests were carried out to compare the vanadium free and vanadium containing steels. Even within the limited scope of these tests, the benefit of the acicular ferrite microstructure to the toughness of the steel was apparent. Table 3 indicates the higher fracture energy of the vanadium containing steel with an acicular ferrite microstructure, compared with the vanadium free steel with a coarser bainitic structure, at the same hardness level. On the corresponding fracture surfaces the vanadium free steel exhibited large areas of cleavage, whereas the vanadium containing steel was mainly ductile.

Discussion

To produce the fine, interwoven platelet structure characteristic of acicular ferrite, it would appear that two criteria are necessary: first, a number of intragranular nucleation events are required, and second, this nucleation gives rise to multiply oriented plate variants (at large angles to each other) so that the chaotic interlocking structure evident in Fig. 1 is produced. To account for the possibility that not every ferrite plate might be nucleated by an inclusion, other

Table 2 Scanning transmission electron microscopy–energy dispersive X-ray (STEM–EDX) analysis results: bulk V content is 0·0053 (mole fraction) for 0·5%V steel

Number	$\{V\}_b$	$\{V\}_\alpha$	Scanned area width, nm	Γ_b^V, atoms/nm^2	Monolayer (V)
1	0·74	0·61	75	8·77	0·45
2	0·83	0·68	37·5	4·64	0·24
3	0·55	0·44	37·5	3·57	0·18
4	0·68	0·40*	20	4·98	0·26
5	0·84	0·52*	20	5·62	0·29
6	0·63	0·52*	20	1·93	0·10
7	0·74	0·36*	20	6·75	0·35
8	0·74	0·70*	20	0·81	0·04
9	0·93	0·55*	20	6·77	0·35
10	0·58	0·43*	20	2·71	0·14
11	0·81	0·56*	20	4·49	0·23
Average	0·73	0·52		4·64	0·24

*Average of analysis of ferrite plates on both sides of ferrite plate boundary.

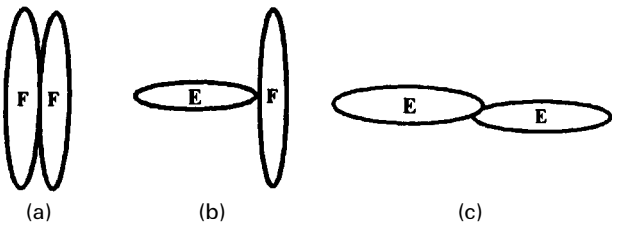

a face to face; b edge to face; c edge to edge

10 Geometries of sympathetic nucleation: after Ref. 14

secondary nucleation events such as 'sympathetic nucleation' or 'autocatalytic nucleation' have been invoked, whereby a ferrite plate can nucleate another, and thus transform the volume of austenite between inclusions (for example, Refs. 14 and 19). Early studies provided metallographic evidence for Widmanstätten ferrite plates nucleating on each other, and also for multiple variants nucleating at inclusions, giving rise to so called 'Widmanstätten stars'.[14] The geometry of sympathetic nucleation, giving rise to plates of parallel orientations, or more oblique orientations, was described by the terms 'face to face', or 'edge to face', respectively,[14] as illustrated in Fig. 10. It follows that sympathetic nucleation to construct an interwoven acicular ferrite microstructure must occur by a preponderance of 'edge to face' type geometry.

A bainitic structure, with no acicular ferrite, was mainly produced in the low oxygen–high nitrogen, vanadium free steel, containing only MnS inclusions, which implies that these MnS inclusions are not an effective nucleant for ferrite, or only a weak nucleant. This view is reinforced by observations in the vanadium treated steels, where the MnS based inclusions within acicular ferrite regions were only ever associated with a single plate variant. The Si–Mn oxide inclusions in the high oxygen–low nitrogen steels appeared to be a more effective ferrite nucleant, but the majority of these inclusions still showed a 1 : 1 inclusion–variant plate relationship, and they too failed to modify the ferrite morphology from bainite to acicular ferrite in the vanadium free steel. Micrographs published in the literature also reveal inclusions within bainitic areas (for example, Refs. 18 and 32). Therefore, the observations suggest that the formation of acicular ferrite in the vanadium treated steels used in the present study is a vanadium effect rather than a direct inclusion effect.

However, this vanadium effect might still be connected with inclusion assisted nucleation of ferrite. The importance of vanadium in nucleating ferrite intragranularly is mentioned above in terms of an inclusion nucleation mechanism, whereby vanadium develops or enhances the nucleation potential of sulphide or oxide inclusions by the precipitation of VN at the inclusion interface; the nitride then nucleates the ferrite with which it produces a low energy interface. Models exist for MnS+ VN (Ref. 29) and Ti_2O_3+ TiN+ V(C,N).[30] However, little vanadium precipitation occurred in the present study owing to a relatively fast cooling rate of approximately 4–11 K s^{-1}, compared with, for example, 0·1 K s^{-1} producing MnS+ VN.[29] Moreover, in all the vanadium treated steels, no vanadium was detected in the inclusions, except that a MnS+ V(C,N) compound was occasionally observed, but only in the low oxygen–high nitrogen 0·5%V steel. Additionally, as

Table 3 Vickers hardness, and impact energy at −20°C

	Hardness, HV10	Impact energy, J
V free steel (V-00)	152±2	12·5
V containing steel (V-10)	153±3	31·5

discussed above, the inclusions in these experimental steels did not appear to be strong ferrite nucleants.

It is important to note that there is likely to be a difference between the inclusions appearing in the present study and those in commercial weld metals. In the present study, the inclusions were simpler than those generally found in commercial steels, which are usually multiphase inclusions (for example, Ref. 10). From the present results, therefore, it is not possible to disregard the effectiveness of complex multiphase inclusions in nucleating intragranular ferrite, and therefore possibly promoting an acicular ferrite microstructure. However, the apparent inertness or weakness of the inclusions in the experimental steels used for the present study meant that any possible alternative influence of the vanadium addition on intragranular ferrite formation was not obscured.

Segregation of vanadium was detected within the fully transformed acicular ferrite microstructures, both at the prior austenite grain boundaries and in the austenite grain interiors. It is not expected that this pattern of substitutional atom segregation would have changed a great deal owing to the relatively rapid cooling rate employed, or during decomposition of the austenite. The higher concentration of vanadium at the prior austenite grain boundaries, indicated by SIMS, may be interpreted as contributing to intragranular acicular ferrite formation, in the present case possibly by suppressing the grain boundary reaction, i.e. preventing the nucleation of coarse grain boundary plate structure. It has been reported[17,33] that the promotion of grain boundary ferrite will encourage intragranular acicular ferrite nucleation, provided that it is inert, i.e. does not develop into coarse Widmanstätten or bainitic ferrite, and it has earlier been suggested[28] that vanadium might have this effect. However, in the present study, regions of coarse, bainitic type ferrite were still observed to develop from the grain boundary ferrite in the vanadium containing steels (Fig. 3), and so it does not appear, at least under the experimental conditions employed, that the grain boundary ferrite was rendered inert by the vanadium additions. However, even if there were some suppression of the grain boundary reaction, acicular ferrite plates needed to be nucleated in the grain interiors in the vanadium containing steels, and in the present study this appeared to occur largely without evidence for strong inclusion assistance, especially if comparison is made with the vanadium free steels.

Accordingly, it is necessary to address the likelihood of an alternative mechanism of intragranular ferrite nucleation, and how this might be enhanced by vanadium alloying. The presence of vanadium segregation within prior austenite grain interiors may be of importance in this. Observations made in other vanadium containing steels are not inconsistent with this segregation; in the untransformed, retained austenite regions of high manganese steels, atom probe field ion microscopy studies[34] have also revealed vanadium atom clustering. Thus, it could be suggested that Fe–V clusters, or regions richer in vanadium than the bulk concentration, might provide suitable sites for the operation of structural embryos appropriate to acicular ferrite nucleation, and so help to explain the vanadium effect. Either the efficacy of inclusion nucleation could be increased, or the effectiveness of sympathetic or autocatalytic nucleation could be increased. A higher vanadium concentration was consistently measured at the plate boundaries, not incompatible with the possible location of plate origins by sympathetic or autocatalytic nucleation as illustrated by Fig. 10. These suggestions are not implausible when it is recognised that vanadium is a ferrite stabiliser; the Fe–V equilibrium diagram displays a γ-loop at the iron rich end,[35] similar to the more familiar Fe–Cr diagram. The energy required to transform to the bcc ferrite state would thus be expected to be lower in a cluster, or region of the fcc Fe–C lattice, rich in vanadium.

Conclusions

1. The intragranular nucleation of ferrite to produce an acicular ferrite microstructure in C–Mn steels has been obtained.
2. The acicular ferrite microstructure appeared to develop principally as a result of vanadium alloying.
3. The intragranular inclusion population appeared to be inert, or only to exert a small direct influence on intragranular ferrite nucleation.
4. Evidence for the segregation of vanadium to the prior austenite grain boundary region, and also in the prior austenite grain interiors, has been found.
5. It has been considered that segregation of vanadium to the prior austenite grain boundaries may cause suppression of the grain boundary reaction to produce coarse, bainitic type ferrite, but observations showed that this was still possible in the vanadium containing steels.
6. In consequence, the possibility has been suggested that intragranular vanadium segregation, to form clusters or regions rich in vanadium, may facilitate intragranular ferrite nucleation, by reducing the energy required for transformation to the bcc state at structural embryos within these regions, either associated with inclusions or with sympathetic/autocatalytic nucleation.
7. Higher impact toughness of the vanadium containing steels with a predominantly acicular ferrite microstructure was observed.

Acknowledgements

This work was funded under Engineering and Physical Sciences Research Council (EPSRC) grant GR/L59511. The authors are grateful to Dr R. M. D. Brydson for advice and assistance with microanalytical TEM.

References

1. J. G. GARLAND and P. R. KIRKWOOD: *Met. Constr.*, 1975, **7**, 275.
2. D. J. ABSON, R. E. DOLBY, and P. H. M. HART: 'Trends in steels and consumables for welding', 75; 1979, Abington, Cambridgeshire, UK, TWI.
3. Y. ITO and M. NAKANISHI: *Sumitomo Search*, 1976, **15**, 42.
4. G. S. BARRITTE and D. V. EDMONDS: 'Advances in the physical metallurgy and applications of steels', 126; 1982, London, The Metals Society.
5. F. ISHIKAWA, T. TAKAHASHI, and T. OCHI: in 'Solid–solid phase transformations', (ed. W. C. Johnson *et al.*), 71; 1994, Warrendale, PA, TMS.
6. R. A. RICKS, P. R. HOWELL, and G. S. BARRITTE: *J. Mater. Sci.*, 1982, **17**, 732.
7. J. M. GREGG and H. K. D. H. BHADESHIA: *Acta Metall. Mater.*, 1994, **42**, 3321.
8. J. M. GREGG and H. K. D. H. BHADESHIA: *Acta Mater.*, 1997, **45**, 739.
9. H. MABUCHI, R. UEMORI, and M. FUJIOKA: *ISIJ Int.*, 1996, **36**, 1406.
10. J. M. DOWLING, J. M. CORBETT, and H. W. KERR: *Metall. Trans. A*, 1986, **17A**, 1611.
11. G. L. F. POWELL, P. G. LLOYD, and J. V. BEE: *Sci. Technol. Weld. Joining*, 1998, **3**, 10.
12. F. J. BARBARO, P. KRAUKLIS, and K. E. EASTERLING: *Mater. Sci. Technol.*, 1989, **5**, 1057.
13. H. K. D. H. BHADESHIA: 'Bainite in steels', 267; 1992, London, The Institute of Metals.
14. H. I. AARONSON and C. WELLS: *Trans. AIME*, 1956, **206**, 1216.
15. G. THEWLISS, J. A. WHITEMAN, and D. J. SENOGLES: *Mater. Sci. Technol.*, 1997, **13**, 257.
16. J. R. YANG and H. K. D. H. BHADESHIA: in 'Welding metallurgy and structural steels', (ed. Y. Koo), 549; 1987, Warrendale, PA, TMS.

17. A. A. B. SUGDEN and H. K. D. H. BHADESHIA: *Metall. Trans. A*, 1998, **20A**, 1811.
18. S. S. BABU and H. K. D. H. BHADESHIA: *Mater. Sci. Technol.*, 1990, **6**, 1005.
19. J. R. YANG and H. K. D. H. BHADESHIA: *Mater. Sci. Technol.*, 1989, **5**, 93.
20. K. YAMAMOTO, S. MATSUDA, T. HAZE, R. CHIJIIWA, and H. MIMURA: in 'Residual and unspecified elements in steel', (ed. A. S. Melilli and E. G. Nisbett), STP 1042, 266; 1989 Philadelphia, PA, ASTM.
21. K. NISHIOKA, H. TAMEHIRO, and M. MURATA: US patent no. 4851052, Washington, DC, 1989.
22. I. MADARIAGA and I. GUTIERREZ: *Mater. Sci. Forum*, 1995, **284**, 419.
23. R. KIRKWOOD and J. G. GARLAND: *Weld. Met. Fabr.*, 1977, **17**
24. A. H. KOUKABI, T. H. NORTH, and H. B. BELL: *Met. Constr.*, 1979, **11**, 639.
25. P. S. MITCHELL, P. H. M. HART, and W. B. MORRISON: Proc. Conf. Microalloying '95, Pittsburgh, PA, USA, ISS, 1995.
26. P. H. M. HART and P. S. MITCHELL: *Weld. Res. (Suppl.)*, 1995, **74**, 239.
27. N. E. HANNERZ and B. M. JONSSON-HOLMQUIST: *Met. Sci.*, 1974, **8**, 228.
28. M. ZHANG and D. V. EDMONDS: in 'HSLA steels '95', (ed. L. Guoxon *et al.*), 133; 1995, Beijing, China Science and Technology Press.
29. F. ISHIKAWA, T. TAKAHASHI, and T. OCHI: *Metall. Mater. Trans. A*, 1994, **25A**, 929.
30. K. YAMAMOTO, S. YOSHIDA, and K. WATANABE: US Patent no. 5421920, Washington, DC, 1995.
31. J. A. S. IKEDA, Y.-M. CHIANG, A. J. GARRATT-REED, and J. B. VANDER SANDE: *J. Am. Ceram. Soc.*, 1993, **76**, 2447.
32. J. R. YANG and H. K. D. H. BHADESHIA: *J. Mater. Sci.*, 1991, **26**, 839.
33. S. S. BABU and H. K. D. H. BHADESHIA: *Mater. Trans., JIM*, 1991, **32**, 679.
34. F. A. KHALID and D. V. EDMONDS: *Mater. Sci. Technol.*, 1993, **9**, 384.
35. O. KUBASCHEWSKI: 'Iron-binary phase diagrams', 160; 1982, New York, Springer-Verlag.